NUCLEAR SCIENCE AND ENGINEERING: 21, 498-508 (1965)

Anisotropic Scattering Approximations in the Monoenergetic Boltzmann Equation*

K. D. Lathrop

University of California, Los Alamos Scientific Laboratory, Los Alamos, New Mexico

Received July 20, 1964
Revised October 15, 1964

The effects of anisotropic scattering approximations in the monoenergetic transport equation are evaluated by calculating discrete eigenvalues, fluxes due to a plane source, and slab critical half-thicknesses, all for homogeneous media. Relative to P_2 scattering approximation results, which are deemed accurate because of their agreement with P_4 solutions, the simple transport approximation overestimates eigenvalues and underestimates half-thicknesses in multiplying media while a P_1 scattering approximation underestimates eigenvalues and overestimates thicknesses, but with smaller error. In the plane source problem, where the detailed flux behavior is observed, the transport approximation is even less accurate; but an extended transport approximation is found to be much more adequate. In overall effectiveness, in order of increasing accuracy, the approximations considered are ranked as follows: 1) transport, 2) forward-backward, 3) first-order Legendre, 4) extended transport, and 5) higher order Legendre. Some evidence is given to indicate that, even for severely anisotropic scattering, relatively low-order Legendre approximations are sufficient to include anisotropic scattering effects.

INTRODUCTION

In numerical solutions of the multigroup transport equation, the general treatment of anisotropic scattering represents a complication that is frequently unwarranted when judged in terms of the effects of anisotropic scattering on solutions. Nevertheless, in certain situations these effects can be important[1,2] and scattering approximations are commonly used to include at least a portion of these effects. While the efficacy of certain scattering approximations has been evaluated in specific, complex problems[1,3], in general the user of a scattering approximation has no guide to its accuracy. This work attempts to provide such a guide by measuring the effectiveness with which several scattering approximations calculate, for the monoenergetic Boltzmann equation, 1) the discrete eigenvalues (diffusion lengths), 2) the flux due to a plane source in an infinite medium and 3) slab critical thicknesses. The generality (and complexity) of energy dependence is sacrificed in order to obtain analytic results in simple systems in which the nature of the scattering approximation is the only variable. In what follows, most numerical results are obtained using the anisotropic scattering coefficients of hydrogen elastic scattering[4], a simple example of scattering anisotropy sufficient to provide a clear separation of results. No restriction on the qualitative nature of the results is incurred.

SCATTERING APPROXIMATIONS

In an infinite, homogeneous, source-free medium containing an isotropic scatterer (Σ_s^{iso}), a fissionable material ($\nu\Sigma_f$), and an anisotropic scat-

*Work performed under the auspices of the USAEC.

[1]G. D. JOANOU and A. H. KAZI, *Trans. Am. Nucl. Soc.* 6, 17 (1963).
[2]B. W. COLSTON, *Trans. Am. Nucl. Soc.* 6, 50 (1963).
[3]H. C. HONECK, *Nucl. Sci. Eng.*, 18, 49 (1964).
[4]B. DAVISON and J. B. SYKES, *Neutron Transport Theory*, Oxford (1957).

terer (Σ_s^{aniso}), the applicable neutron transport equation is

$$\mu\frac{\partial\Psi(x,\mu)}{\partial x} + \Sigma_t\Psi(x,\mu) = \frac{\Sigma_s^{iso} + \nu\Sigma_f}{2}\int_{-1}^{1}\Psi(x,\mu')d\mu' +$$

$$+ \Sigma_s^{aniso}\iint\Psi(x,\mu')\,f(\vec{\Omega}'\cdot\vec{\Omega})\,d\Omega', \quad (1)$$

where

$\Psi(x,\mu)$ is the neutron angular flux and

f is the scattering function for transfers between initial directions $\vec{\Omega}'$ to final directions in $d\Omega = d\mu d\phi$ about $\vec{\Omega}$.

If f is assumed to depend only upon the angle between initial and final neutron directions (a not very restrictive assumption), Ψ is independent of ϕ; and a general representation of the scattering function is

$$f(\vec{\Omega}'\cdot\vec{\Omega}) \equiv f(\mu_0) = \sum_{n=0}^{\infty}\frac{2n+1}{4\pi}\,b_n\,P_n\,(\mu_0), \quad (2)$$

where the P_n are Legendre polynomials. Using Eq. (2) the ϕ' integration of Eq. (1) gives

$$\mu\frac{\partial\Psi(x,\mu)}{\partial x} + \Sigma_t\Psi(x,\mu) = \frac{(\Sigma_s^{iso} + \nu\Sigma_f)}{2}\Psi_0(x) +$$

$$+ \Sigma_s^{aniso}\sum_{n=0}^{\infty}\frac{2n+1}{2}\,b_n\,P_n(\mu)\Psi_n(x), \quad (3)$$

where $\Psi_n(x)$ is the n'th Legendre moment of $\Psi(x,\mu)$. Assuming a separable flux of the form

$$\Psi(x,\mu) = e^{-\Sigma_t x\lambda}\,\varphi(\mu), \quad (4)$$

abbreviating the isotropic secondaries ratio as

$$c' = (\nu\Sigma_f + \Sigma_s^{iso})/\Sigma_t \quad (5)$$

and the anisotropic scattering ratio as

$$c = \Sigma_s^{aniso}/\Sigma_t, \quad (6)$$

and substituting in Eq. (3) gives an equation for the angular dependence of the flux

$$(1-\mu\lambda)\varphi(\mu) = c\sum_{n=0}^{\infty}\frac{2n+1}{2}\,\tilde{b}_n\,P_n\,(\mu)\,\varphi_n. \quad (7)$$

In Eq. (7) the φ_n are the Legendre moments of $\varphi(\mu)$ and

$$\tilde{b}_0 = 1 + c'/c,\ \tilde{b}_n = b_n,\ n>0. \quad (8)$$

If, on the basis of small scattering function expansion coefficients or of small flux moments or both, the terms of the series in Eq. (7) are assumed to be negligible for $n > N$ the resulting approximation is known as the P_N scattering approximation. In this case, the angular flux is approximated by

$$\varphi(\mu) = \frac{c\sum_{n=0}^{N}\frac{2n+1}{2}\,\tilde{b}_n\,P_n\,(\mu)\,\varphi_n}{1-\mu\lambda}. \quad (8)$$

The φ_n are defined recursively by multiplying Eq. (7) by P_n and integrating to give

$$(n+1)\varphi_{n+1} = (2n+1)\,(1 - c\tilde{b}_n)\varphi_n/\lambda - n\varphi_{n-1},$$

$$n \le N \quad (9a)$$

$$(n+1)\varphi_{n+1} = (2n+1)\varphi_n/\lambda - n\varphi_{n-1},$$

$$n \ge N. \quad (9b)$$

For $\lambda \in [-1, 1]$ normalizing $\varphi(\mu)$ to unity determines the discrete eigenvalues as those $\lambda = \lambda_i$ which are solutions of

$$1 = \frac{c}{\lambda}\sum_{n=0}^{N}(2n+1)\,\tilde{b}_n\varphi_n\left(\frac{1}{\lambda}\right)Q_n\left(\frac{1}{\lambda}\right), \quad (10)$$

where

Q_n are the associated Legendre functions[5].

For $N = 0$ Eq. (10) is the familiar eigenvalue equation for isotropic scattering

$$\lambda = (c + c')\tanh^{-1}\lambda. \quad (11)$$

Mika[6] has shown that there are at most $N+1$ pairs (plus or minus λ_i) of roots to Eq. (10) including the possibility of $\lambda_i \notin [-1, 1]$ corresponding to diffusion lengths shorter than a mean free path. Some conditions (on c and the b_n) for the existence of only one pair of solutions to Eq. (10) are given in the appendix of Ref. 7. Since the transport approximation ($N = 0$) gives only one pair of solutions, while P_N approximation with the $\tilde{b}_n$ assumed by the transport approximation can have more than one pair of solutions, the implication is that the additional solutions are due to the nature of the finite polynomial approximation. Here, only the smallest λ_i of Eq. (10) will be calculated.

If, instead of truncating the scattering expansion at $n = N$, all the $\tilde{b}_n$ for $n > N$ are assumed to be given by $\tilde{b}_n = a_1 + (-1)^n a_2$, the scattering approximation is an N term Legendre expansion plux a forward scattering component of strength

[5] A. ERDELYI, editor, *Higher Transcendental Functions*, 1, p. 152 McGraw-Hill (1953).

[6] JANUSZ R. MIKA, *Nucl. Sci. Eng.*, 11, 415 (1961).

[7] K. D. LATHROP, "Anisotropic Scattering Approximations in the Boltzmann Transport Equation," Los Alamos Scientific Laboratory Report LA-3051 (1964).

a_1 and a backward scattering component of strength a_2. The angular flux components are still defined by Eq. (9a) for $n \leq N$, but are given by

$$(n+1)\varphi_{n+1} = (2n+1)\,[1 - c(a_1 + (-1)^n a_2)] \times \times \varphi_n/\lambda - n\varphi_{n-1}, \quad (12)$$

when $n > N$. If the strengths of the forward and backward components are chosen to satisfy the $N+1$ and $N+2$ moments of the scattering function of Eq. (2)

$$\tilde{b}_{N+1} = a_1 + (-1)^{N+1} a_2$$
$$\tilde{b}_{N+2} = a_1 + (-1)^{N+2} a_2, \quad (13)$$

then Eq. (12) will have the same form as Eq. (9a) for $n = N+1$ and $n = N+2$. The eigenvalue equation for this scattering approximation is given by Eq. (10) with the following replacements:

$$\lambda \rightarrow \lambda/[(1 - c\tilde{b}_{N+1})(1 - c\tilde{b}_{N+2})]^{\frac{1}{2}}$$

$$\text{even } N\text{: } \tilde{b}_n \rightarrow \frac{\tilde{b}_n - \tilde{b}_{N+2}}{1 - c\tilde{b}_{N+2}} \text{ even } n$$

$$\tilde{b}_n \rightarrow \frac{\tilde{b}_n - \tilde{b}_{N+1}}{1 - c\tilde{b}_{N+1}} \text{ odd } n$$

$$\text{odd } N\text{: } \tilde{b}_n \rightarrow \frac{\tilde{b}_n - \tilde{b}_{N+1}}{1 - c\tilde{b}_{N+1}} \text{ even } n$$

$$\tilde{b}_n \rightarrow \frac{\tilde{b}_n - \tilde{b}_{N+2}}{1 - c\tilde{b}_{N+2}} \text{ odd } n\,. \quad (14)$$

For $N = 0$ the above formalism results in a modified form of the isotropic eigenvalue equation, here called the forward-backward (FB) approximation. The simple transport approximation (TR) is obtained by setting the coefficient of the backward scattering component to zero so that all $\tilde{b}_n$, $n > 0$, are assumed equal to $a_1 = \tilde{b}_1$. The resulting eigenvalue equation is

$$1 = \frac{c(\tilde{b}_0 - \tilde{b}_1)}{\lambda} \tanh^{-1} \frac{\lambda}{1 - c\tilde{b}_1}\,. \quad (15)$$

In Eq. (15), as well as in more general problems, the TR approximation consists of a simple adjustment of cross sections which permits an isotropic-type solution. This simplicity does not apply to the FB approximation because of the square root in Eq. (14). However, the FB approximation may serve in analytic investigations in which effects of anisotropic scattering are to be included although the continuous eigenfunctions ($\lambda \notin [-1, 1]$) are not of the simple isotropic form. The transport-type approximation may be made with any order P_N approximation. Here an extended transport approximation ($EXTR$) obtained by adjusting the cross sections of the P_1 approximation ($N = 1$, $a_2 = 0$ in Eq. (14)) is examined.

Other scattering approximations are possible. The transfer function, Eq. (2), may be approximated by combinations of step functions. While such combinations can adequately predict discrete eigenvalues[8], these approximations are not simply applied unless a matrix of scattering transfer coefficients is prepared. In this case direct use of the scattering function, as in a Monte Carlo calculation, appears more feasible.

EIGENVALUES

Using Eq. (10) and its modifications, eigenvalues were calculated for the P_N, TR, FB, and $EXTR$ approximations for a variety of values of c and c' using the b_n for elastic hydrogen scattering. Table I shows the eigenvalues for purely anisotropic scattering ($c' = 0$) while Table II displays eigenvalues for a small anisotropic scattering ratio ($c = 0.1$) and Table III displays eigenvalues for a large anisotropic scattering ratio ($c = 0.9$). In Tables II and III c' was taken in the range $0 \leq c' < (1 - c)\nu$ with $\nu = 2.5$ and the magnitude of imaginary eigenvalues ($c + c' > 1.0$) is entered. In computation of discrete eigenvalues with hydrogen anisotropic scattering, P_2 eigenvalues are sufficiently close to P_4 eigenvalues to be used as a standard of comparison. (The P_4 eigenvalues are essentially exact, agreeing with eigenvalues calculated by direct solution of the integral equation using the exact scattering kernel[8].) Figures 1 through 5 display the percentage deviation from P_2 eigenvalues for five values of the anisotropic scattering ratio. More extensive tables of eigenvalues, $c = 0.5$ (0.05) 0.95, and percentage deviation plots, $c = 0.1$ (0.1) 0.90, 0.95 are given in Ref. 7.

For small anisotropic scattering ratios (Fig. 1) all approximations give results within a percent of P_2 values when $c + c'$ is greater than unity; but for large absorption ratios, the TR, FB and $EXTR$ approximations are poor. These approximations, which in one form or another imply an increased scattering mean free path before scattering with a reduced effective secondaries ratio ($c + c' < 1$), distort the physical process. For example, when $c + c'$ is small, λ in the P_N approximations differs from unity by a small term of order exponential $[-2/(c + c')\alpha_N]$. For the TR approximation in the same situation Eq. (15) is an equation for $\lambda/(1 - cb_1)$ with an effective secondaries ratio $(c + c' - cb_1)/(1 - cb_1)$ which is less than $c + c'$ when

[8] K. D. LATHROP, "Anisotropic Scattering in the Transport Equation," Los Alamos Scientific Laboratory Report LAMS-2873 (1963).

TABLE I

Discrete Eigenvalues for Anisotropic Scattering Approximations *

$c' = 0$

Anisotropic Scattering Ratio	Scattering Approximation						
c	Isotropic	Transport	Forward-Backward	Extended Transport	P_1	P_2	P_4
0.05	1.0000	0.9667	0.9770	0.9875	1.0000	1.0000	
0.10	1.0000	0.9333	0.9539	0.9750	0.9996	0.9982	0.9985
0.15	1.0000	0.9000	0.9307	0.9619	0.9957	0.9904	
0.20	0.9999	0.8667	0.9074	0.9468	0.9860	0.9759	0.9767
0.25	0.9993	0.8333	0.8839	0.9285	0.9700	0.9556	
0.30	0.9974	0.8000	0.8598	0.9065	0.9482	0.9305	0.9312
0.35	0.9932	0.7667	0.8348	0.8807	0.9212	0.9012	
0.40	0.9856	0.7333	0.8083	0.8511	0.8896	0.8682	0.8687
0.45	0.9740	0.6999	0.7796	0.8179	0.8536	0.8318	
0.50	0.9575	0.6662	0.7481	0.7811	0.8137	0.7921	0.7924
0.55	0.9355	0.6321	0.7134	0.7407	0.7698	0.7492	0.7494
0.60	0.9073	0.5969	0.6751	0.6967	0.7222	0.7031	0.7032
0.65	0.8721	0.5603	0.6325	0.6490	0.6706	0.6535	0.6536
0.70	0.8286	0.5212	0.5853	0.5971	0.6149	0.6002	0.6002
0.75	0.7755	0.4788	0.5328	0.5406	0.5547	0.5426	0.5426
0.80	0.7104	0.4313	0.4738	0.4785	0.4889	0.4796	0.4796
0.85	0.6295	0.3766	0.4068	0.4092	0.4162	0.4097	0.4097
0.90	0.5254	0.3102	0.3281	0.3290	0.3330	0.3292	0.3292
0.95	0.3795	0.2214	0.2283	0.2285	0.2299	0.2285	0.2285
0.97	0.2964				0.1762	0.1755	0.1755
0.99	0.1725				0.1006	0.1005	0.1005

* Hydrogen elastic scattering, $b_0 = 1$, $b_1 = \frac{2}{3}$, $b_2 = \frac{1}{4}$, $b_3 = 0$, $b_4 = -\frac{1}{24}$

TABLE II

Discrete Eigenvalues for Scattering Approximations*

$c = 0.1$

Isotropic Secondaries Ratio	Scattering Approximation					
c'	Isotropic	P_1	P_2	Transport	Forward-Backward	Extended Transport
0.1	1.0000	0.9967	0.9937	0.9333	0.9539	0.9742
0.2	0.9974	0.9878	0.9833	0.9327	0.9523	0.9691
0.3	0.9856	0.9686	0.9635	0.9262	0.9428	0.9544
0.4	0.9575	0.9349	0.9299	0.9051	0.9179	0.9248
0.5	0.9073	0.8817	0.8777	0.8626	0.8716	0.8752
0.6	0.8286	0.8028	0.8000	0.7918	0.7974	0.7990
0.7	0.7104	0.6871	0.6855	0.6817	0.6847	0.6852
0.8	0.5254	0.5077	0.5072	0.5060	0.5071	0.5071
0.9	0.0	0.0	0.0	0.0	0.0	0.0
1.0	0.5693	0.5501	0.5506	0.5514	0.5505	0.5506
1.1	0.8345	0.8068	0.8082	0.8102	0.8077	0.8080
1.2	1.0571	1.0225	1.0251	1.0284	1.0238	1.0246
1.3	1.2598	1.2195	1.2232	1.2277	1.2209	1.2225
1.4	1.4511	1.4058	1.4108	1.4163	1.4071	1.4097
1.5	1.6350	1.5853	1.5915	1.5980	1.5862	1.5900
1.6	1.8138	1.7601	1.7675	1.7749	1.7604	1.7656
1.7	1.9888	1.9316	1.9402	1.9484	1.9311	1.9378
1.8	2.1611	2.1006	2.1104	2.1192	2.0991	2.1075
1.9	2.3311	2.2677	2.2786	2.2881	2.2651	2.2752
2.0	2.4994	2.4333	2.4453	2.4553	2.4294	2.4415
2.1	2.6664	2.5977	2.6108	2.6213	2.5923	2.6065
2.2	2.8322	2.7612	2.7753	2.7862	2.7542	2.7705

* Hydrogen elastic scattering

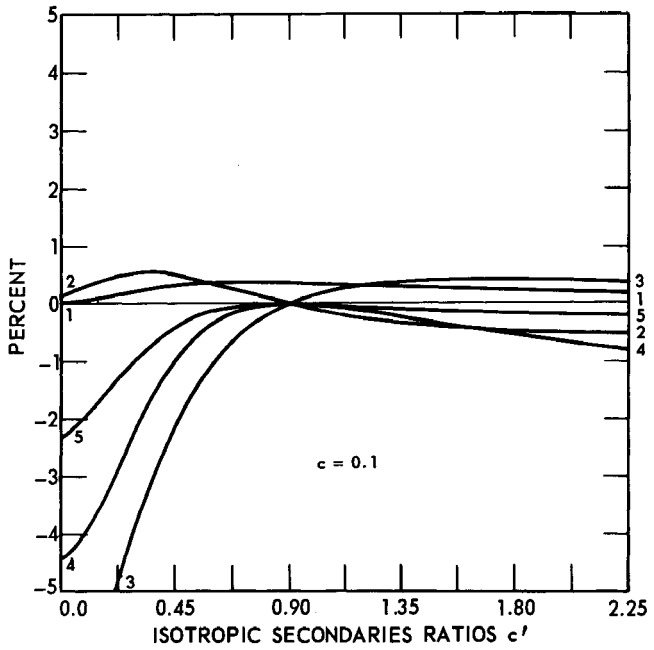

Fig. 1. Percentage deviation from P_2 eigenvalues as a function of the isotropic secondaries ratio. Scattering approximations: 1) ISOTROPIC (times 1/10), 2) P_1, 3) TRANSPORT, 4) FORWARD-BACKWARD, 5) EXTENDED TRANSPORT.

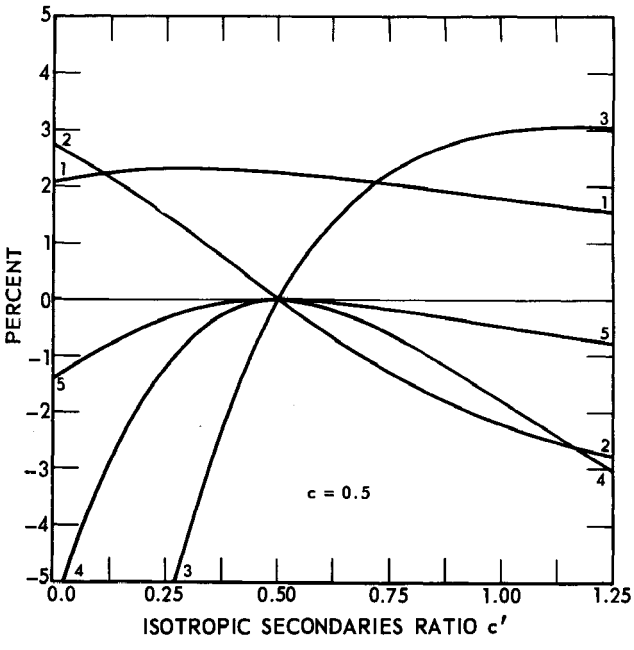

Fig. 3. Percentage deviation from P_2 eigenvalues as a function of the isotropic secondaries ratio. Scattering approximations: 1) ISOTROPIC (times 1/10), 2) P_1, 3) TRANSPORT, 4) FORWARD-BACKWARD, 5) EXTENDED TRANSPORT.

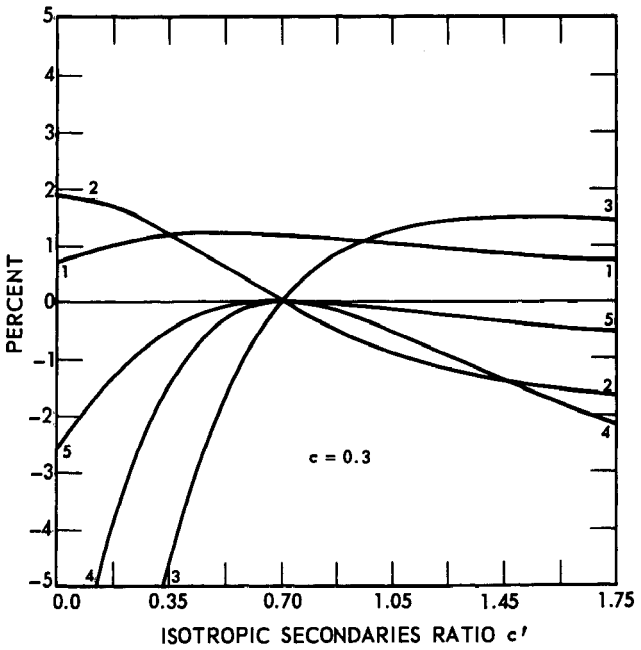

Fig. 2. Percentage deviation from P_2 eigenvalues as a function of the isotropic secondaries ratio. Scattering approximations: 1) ISOTROPIC (times 1/10), 2) P_1, 3) TRANSPORT, 4) FORWARD-BACKWARD, 5) EXTENDED TRANSPORT.

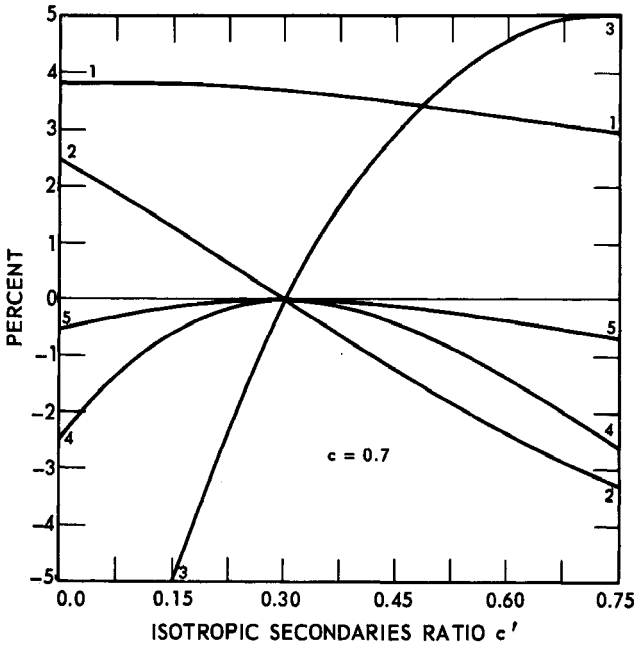

Fig. 4. Percentage deviation from P_2 eigenvalues as a function of the isotropic secondaries ratio. Scattering approximations: 1) ISOTROPIC (times 1/10), 2) P_1, 3) TRANSPORT, 4) FORWARD-BACKWARD, 5) EXTENDED TRANSPORT.

TABLE III

Discrete Eigenvalues for Scattering Approximations *
$c = 0.9$

Isotropic Scattering Ratio	Scattering Approximation					
c'	Isotropic	P_1	P_2	Transport	Forward-Backward	Extended Transport
0.05	0.3795	0.2401	0.2388	0.2324	0.2386	0.2387
0.10	0.0	0.0	0.0	0.0	0.0	0.0
0.15	0.3950	0.2499	0.2514	0.2569	0.2512	0.2514
0.20	0.5693	0.3607	0.3649	0.3797	0.3639	0.3647
0.25	0.7101	0.4508	0.4589	0.4842	0.4561	0.4583

* Hydrogen elastic scattering

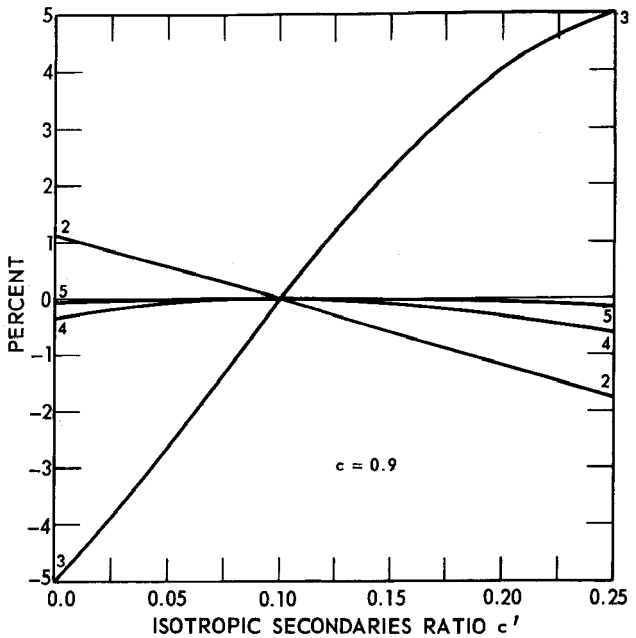

Fig. 5. Percentage deviation from P_2 eigenvalues as a function of the isotropic secondaries ratio. Scattering approximations: 1) ISOTROPIC (times 1/10), 2) P_1, 3) TRANSPORT, 4) FORWARD-BACKWARD, 5) EXTENDED TRANSPORT. (Isotropic error greater than 50%).

$c + c'$ is less than one. Then for $c + c' < 0.3$, $\lambda/(1 - cb_1) \approx 1$ and $\lambda \approx 1 - cb_1 < 1$. Thus for strongly absorbing media the *TR* approximation underestimates λ by just the amount the scattering cross section is decreased. The same type of error occurs with the *FB* and *EXTR* approximations, although with a smaller magnitude. The P_1 approximation, in which the scattering cross section is not altered, is much more accurate in strongly absorbing situations.

As the anisotropic scattering ratio increases, all approximations become worse; and of all the approximations, the *TR* approximation is the poorest except for large values of $c + c'$ and small c when the *FB* and P_1 approximations are somewhat poorer. For $c = 0.7$ (Fig. 4), the *TR* approximation is in error by more than 5% when $c' < 0.15$ or $c' > 0.65$, and the error is worse when c is larger. Thus only when $c + c'$ is near unity or when anisotropic scattering is relatively unimportant is the *TR* approximation accurate.

The *EXTR* approximation is considerably better than the P_1 approximation unless the absorption ratio is high when the *EXTR* approximation makes the same type of error the *TR* approximation does. These results indicate that if anisotropic scattering is important and a *TR* type approximation is to be made, it can profitably be made by adjusting P_1 scattering coefficients. The P_1 approximation itself is surprisingly accurate with errors of more than 3% occurring only at the largest values of c' and these large errors only for intermediate values of c. For almost all values of $c + c'$ the P_1 error is less than 2%.

FLUX IN AN INFINITE, HOMOGENEOUS MEDIUM CONTAINING A PLANE SOURCE

Using the method of eigenfunction expansion, Mika[6] solved the problem of determining the flux in an infinite, homogeneous medium containing a plane source. A P_N approximation was used to represent anisotropic scattering. The same problem was solved by Fourier transforms in Ref. 7. In the plane source problem the contribution to the zeroth Legendre component of the angular flux conveniently separates into a portion due to the discrete eigenfunctions (the asymptotic flux) and a portion due to the continuous eigenfunctions (the transient flux) so that the effect of scattering approximations on the continuous eigenfunctions is easily assessed. The form of the solution with a P_N scattering approximation is given in the notation of Ref. 7, by

$$\Psi_{0_{as}}(x) = e^{-\lambda|x|} \frac{\left\{\left[c\sum_{n=1}^{N}(2n+1)\,\tilde{b}_n\,a_n\,Q_n\left(\frac{1}{\lambda}\right)\right] - Q_0\left(\frac{1}{\lambda}\right)\right\}}{\lambda\frac{d}{d\lambda}\left[1-\frac{c}{\lambda}\sum_{n=0}^{N}(2n+1)\,\tilde{b}_n\,h_n\,Q_n\left(\frac{1}{\lambda}\right)\right]} \tag{16}$$

and

$$\Psi_{0_{tran}}(x) = \frac{1}{2}\int_1^\infty \frac{te^{-|x|t}\,dt}{\left(t + W_h - P_h\,\frac{1}{2}\,\ell n\,\frac{t+1}{t-1}\right)^2 + \left(\frac{\pi P_h}{2}\right)^2}, \tag{17}$$

where h_n and a_n are polynomials satisfying the recursion relation

$$(n+1)\,h_{n+1} = (2n+1)\,(1 - c\tilde{b}_n) \times \times h_n/iw - nh_{n-1}, \tag{18}$$

but $h_0 = 1$, while $a_0 = 0$ and $a_1 = 1/iw$. The term λ is that value of $w = i\lambda_0$ which makes the quantity in brackets in the denominator of Eq. (16) vanish, that is, λ_0 is the discrete eigenvalue of Eq. (10). The denominator of Eq. (16) is a symbolism for the derivative of the quantity in brackets evaluated at a λ_0 such that the quantity in brackets vanishes. The derivative is conveniently evaluated in the process of finding λ_0 by Newton's method. Finally

$$P_h = \sum_{n=0}^{N}(2n+1)\,c\tilde{b}_n\,h_n\left(\frac{1}{t}\right)P_n\left(\frac{1}{t}\right)$$

$$W_h = \sum_{n=1}^{N}(2n+1)\,c\tilde{b}_n\,h_n\left(\frac{1}{t}\right)W_n\left(\frac{1}{t}\right)$$

$$Q_n = P_nQ_0 - W_{n-1}. \tag{19}$$

The forward-backward type scattering approximations are obtained simply by transformations, given in detail in Ref. 7, similar to those of Eq. (14). In particular, if $\Psi_{0_{iso}}(x, \tilde{b}_0)$ is the total isotropic flux of Eq. (16) and (17), the *TR* approximation flux is

$$\Psi_{0_{TR}}(x) = \Psi_{0_{iso}}(x', b_0')$$

$$x' = (1 - c\tilde{b}_1)\,x \tag{20}$$

$$b_0' = (\tilde{b}_0 - \tilde{b}_1)/(1 - c\tilde{b}_1).$$

In Ref. 7 it is shown that the *FB* approximation flux is, relative to the flux at the origin in the P_N approximations, enhanced by the ratio $(1 - c\tilde{b}_1)^{\frac{1}{2}}/(1 - c\tilde{b}_2)^{\frac{1}{2}}$. The enhancement is due to the backward scattering component. In elastic hydrogen scattering there is no backward scattering and use of the *FB* approximation results in a negative backward scattering component which leads to a relative flux depression near the origin.

Fluxes for a purely anisotropic scattering ratio $c = 0.9$, $c' = 0$ are given in Table IV for P_N, *TR*, *FB*, and *EXTR* scattering approximations. In the table the total flux, the eigenvalue λ_0 and the coefficient of the asymptotic flux are given. Much more detailed tables are given in Ref. 7 for $c' = 0$, $c = 0.1\,(0.1)\,0.5\,(0.05)\,0.95\,(0.02)\,0.99$. Plots of the percentage deviations from P_4 fluxes are shown in Figs. 6, 7 and 8 for three values of c. In these figures the deviation of P_2 fluxes from P_4 fluxes is extremely small except near the source plane, indicating that the higher order P_N approximation is needed only when 'transient' effects, in this case, due to the source, are present. Even near the source the P_2 results are within 0.3% of the P_4 fluxes. Again, the *TR* approximation is the worst of those examined. The *TR* fluxes are too large near the origin because of too many scattering contributions directly from the source due to the larger effective scattering mean free path, too small at intermediate distances because the coefficient of the asymptotic flux is too small, and too large at large distances because λ_0 is underestimated. For $c \geq 0.6$ the *FB* approximation is somewhat more accurate than the *TR* approximation except near the source where the *FB* approximation flux does not approach infinity at the same rate as

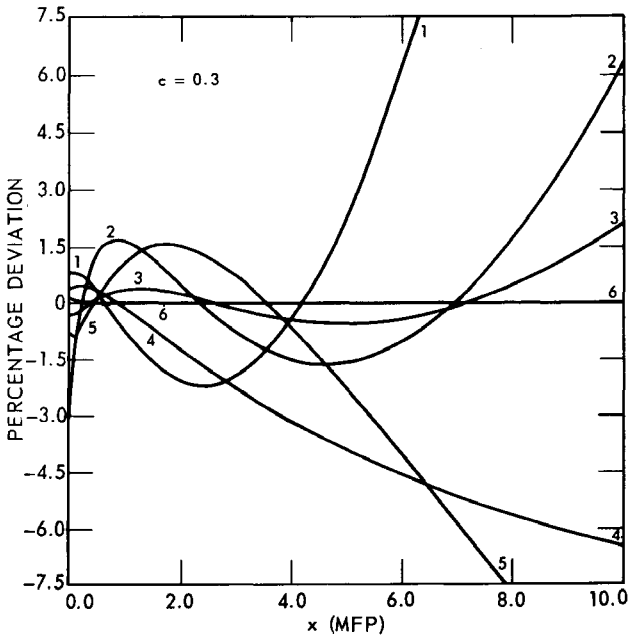

Fig. 6. Percentage deviation from P_4 fluxes as a function of the distance from the source. Scattering approximations: 1) TRANSPORT, 2) FORWARD-BACKWARD, 3) EXTENDED TRANSPORT, 4) ISOTROPIC (times 1/10), 5) P_1, 6) P_2.

TABLE IV

Total Flux (Comparative) for a Plane Source in an Infinite, Homogeneous Medium*
$c' = 0$, $c = 0.9$

Mean Free Path	Scattering Approximation						
x	Transport	Forward-Backward	Extended Transport	Isotropic	P_1	P_2	P_4
0.02	3.2881	2.8030	3.1259	3.9642	3.0499	3.1636	3.1578
0.06	2.7322	2.3992	2.5803	3.3905	2.5105	2.6124	2.6082
0.1	2.4703	2.2066	2.3280	3.1108	2.2637	2.3554	2.3523
0.2	2.1081	1.9353	1.9871	2.7047	1.9346	2.0054	2.0042
0.4	1.7326	1.6433	1.6458	2.2454	1.6114	1.6527	1.6531
0.6	1.5038	1.4571	1.4430	1.9393	1.4215	1.4437	1.4445
0.8	1.3364	1.3157	1.2958	1.7016	1.2837	1.2932	1.2940
1.0	1.2036	1.1999	1.1787	1.5055	1.1734	1.1744	1.1751
1.5	0.9568	0.9755	0.9576	1.1287	0.9622	0.9527	0.9530
2.0	0.7800	0.8068	0.7940	0.8567	0.8026	0.7902	0.7902
4.0	0.3793	0.4007	0.3990	0.2946	0.4060	0.3986	0.3986
6.0	0.1952	0.2051	0.2054	0.1027	0.2082	0.2056	0.2056
8.0	0.1025	0.1058	0.1062	0.0359	0.1069	0.1064	0.1064
10.0	0.0543	0.0548	0.0550	0.0125	0.0549	0.0551	0.0551
ASYMPTOTIC FLUX							
EIGENVALUE[a]	0.7755[b]	0.5893	0.4245	0.5254	0.3330	0.3292	0.3292
COEFFICIENT OF EXPONENT	1.1728	1.4536	1.4763	2.4003	1.5344	1.4810	1.4811

* Hydrogen elastic scattering

[a] λ of $e^{-\lambda|x|}$

[b] Isotropic eigenvalue for $cb'_0 = c(b_0 - b_1)/(1 - cb_1) = 0.75$. Similar eigenvalues are given for the *FB* and *EXTR* approximations

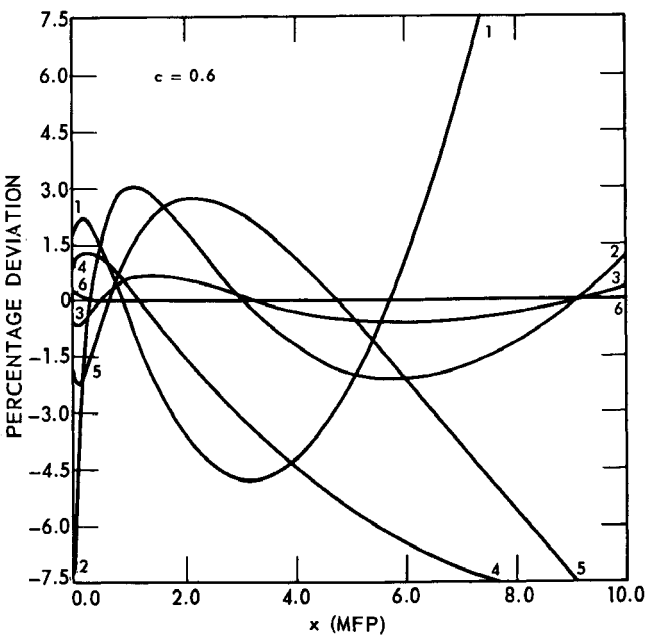

Fig. 7. Percentage deviation from P_4 fluxes as a function of the distance from the source. Scattering approximations: 1) TRANSPORT, 2) FORWARD-BACKWARD, 3) EXTENDED TRANSPORT, 4) ISOTROPIC (times 1/10), 5) P_1, 6) P_2.

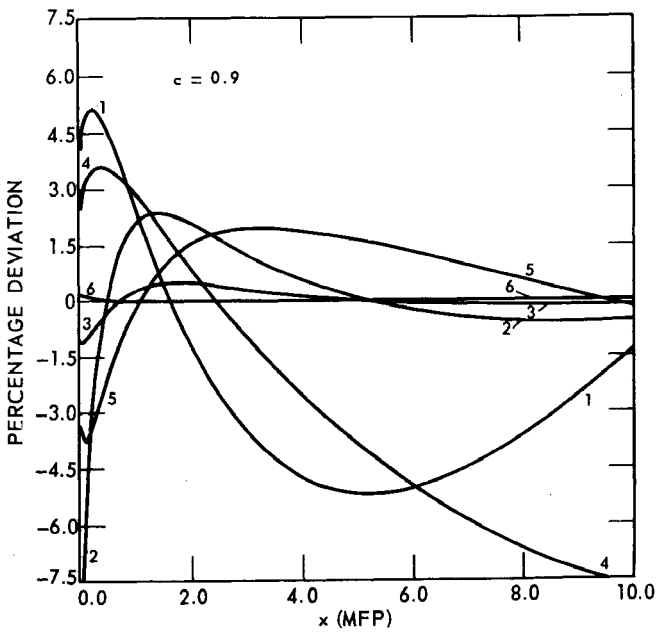

Fig. 8. Percentage deviation from P_4 fluxes as a function of the distance from the source. Scattering approximations: 1) TRANSPORT, 2) FORWARD-BACKWARD, 3) EXTENDED TRANSPORT, 4) ISOTROPIC (times 1/10), 5) P_1, 6) P_2.

the other fluxes. As shown in an examination of an exact solution for the angular flux in a medium with a purely forward-backward scatter[7], if the coefficient of backward scattering is positive, the flux near the source is enhanced by those neutrons which scatter backwards. Since hydrogen scattering is entirely in the forward direction, the coefficient of backward scattering is negative and the *FB* approximation flux is depleted near the origin. These arguments also show that hydrogen scattering is not a fair test of the *FB* approximation, and the relatively good agreement of the *FB* results is simply a consequence of satisfying more angular flux moments. The *EXTR* approximation gives fluxes in excellent agreement with P_4 fluxes except in strongly absorbing media where the underestimation of the discrete eigenvalue causes overestimation of the flux at large distances from the source. The P_1 approximation underestimates fluxes near the source (again due to a negative backward scattering component) and underestimates the flux at large distances from the origin because λ_0 is overestimated, the most serious errors occurring at large distances from the source.

SLAB CRITICAL THICKNESSES

Leonard and Mullikin, using the method of singular integral equations[9] have obtained an exact critical equation for a homogeneous plane slab including an anisotropic scatterer with properties represented by a P_N scattering approximation. Comparisons of numerical solutions of this critical equation and numerical results obtained from an anisotropic scattering approximation modification of the Los Alamos transport code[10] DTF have shown excellent agreement[11]. The critical thicknesses displayed in Table V to IX were calculated using the DTF code. A DP_7 (double P_N approximation equivalent to S_{16}) angular quadrature scheme was used to represent the neutron flux. Percentage deviations from P_2 critical half-thicknesses are plotted in Figs. 9 and 10. The P_2 half-thicknesses are very nearly converged results, that is, increasing the order of the P_N approximation does not significantly change the half-thickness. For hydrogen scattering $b_3 = 0$, so P_2 and P_3 solutions are identical. The coefficient of the P_4 component is $-\frac{1}{24}$ and that of the P_5 component, zero. In the case of $c + c' = 1.4$ and $c = 0.9$ when the greatest deviation between P_1 and P_2 results is observed (3.41%), the P_4 result is 0.83068 compared to the

TABLE VI

Slab Critical Half-Thickness (Mean Free Path)*
$c + c' = 1.1$

Anisotropic Scattering Ratio	Scattering Approximation			
c	Isotropic	Transport	P_1	P_2
0.0	2.1136			
0.1		2.16093	2.16524	2.16311
0.3		2.26702	2.28290	2.27558
0.5		2.39097	2.42452	2.41031
0.7		2.53782	2.59999	2.57637
0.9		2.71345	2.82629	2.78923

*Elastic hydrogen scattering

TABLE V

Slab Critical Half-Thickness (Mean Free Path)*
$c + c' = 1.05$

Anisotropic Scattering Ratio	Scattering Approximation			
c	Isotropic	Transport	P_1	P_2
0.0	3.30036			
0.1		3.38841	3.39225	3.39042
0.3		3.58925	3.60356	3.59724
0.5		3.83304	3.86368	3.85135
0.7		4.13783	4.19568	4.17506
0.9		4.53405	4.64212	4.60935

*Elastic hydrogen scattering

TABLE VII

Slab Critical Half-Thickness (Mean Free Path)*
$c + c' = 1.2$

Anisotropic Scattering Ratio	Scattering Approximation			
c	Isotropic	Transport	P_1	P_2
0.0	1.28940			
0.1		1.31085	1.31521	1.31299
0.3		1.35672	1.37256	1.36498
0.5		1.40661	1.43939	1.42486
0.7		1.45921	1.51884	1.49506
0.9		1.51266	1.61576	1.57930

*Elastic hydrogen scattering

[9]A. LEONARD and T. W. MULLIKIN, "A Spectral Analysis of the Anisotropic Neutron Transport Kernel in Slab Geometry with Applications," *J. Math. Phys.* 5, 399 (1964).

[10]B. G. CARLSON, W. J. WORLTON, W. GUBER and M. SHAPIRO, "DTF Users Manual," United Nuclear Corporation UNC Phys/Math-3321, I (1963).

[11]A. LEONARD, personal communication (May, 1964).

TABLE VIII

Slab Critical Half-Thickness (Mean Free Path)*
$c + c' = 1.3$

Anisotropic Scattering Ratio	Scattering Approximation			
c	Isotropic	Transport	P_1	P_2
0.0	0.937740			
0.1		0.94936	0.95354	0.95142
0.3		0.97315	0.98811	0.98098
0.5		0.99699	1.02747	1.01398
0.7		1.01909	1.07292	1.05123
0.9		1.03512	1.12636	1.09382

*Elastic hydrogen scattering

P_2 result of 0.83022. In these problems the angular neutron flux is relatively isotropic so that the importance of the higher order Legendre components decreases rapidly, regardless of the size of the expansion coefficients, and for hydrogen scattering the expansion coefficients themselves are small.

For plane geometry and values of $c + c'$ near unity, the critical half-thickness is given, to a good approximation, by

$$t/2 = \pi/(2|\lambda_0|) - z_0 , \qquad (21)$$

where z_0 is the Milne problem extrapolation distance properly corrected for anisotropic scattering. For example, for $c + c' = 1.2$ and $c = 0.9$ this formula gives 1.58061 for $t/2$ compared to an exact result[11] of 1.57929 and a DTF result of 1.57930. The formula is even better for smaller values of $c + c'$. Since the *TR* approximation overestimates λ_0 for $c + c' > 1$, it can be expected to underestimate $t/2$ provided there is no compensating change in z_0. The results plotted in Fig. 9 show that the *TR* approximation does indeed underestimate the critical half-thickness. In a similar fashion, the

TABLE IX

Slab Critical Half-Thickness (Mean Free Path)*
$c + c' = 1.4$

Anisotropic Scattering Ratio	Scattering Approximation			
c	Isotropic	Transport	P_1	P_2
0.0	0.73662			
0.1		0.74332	0.74726	0.74532
0.3		0.75633	0.77031	0.76381
0.5		0.76795	0.79607	0.78393
0.7		0.77634	0.82519	0.80595
0.9		0.77756	0.85853	0.83022

*Elastic hydrogen scattering

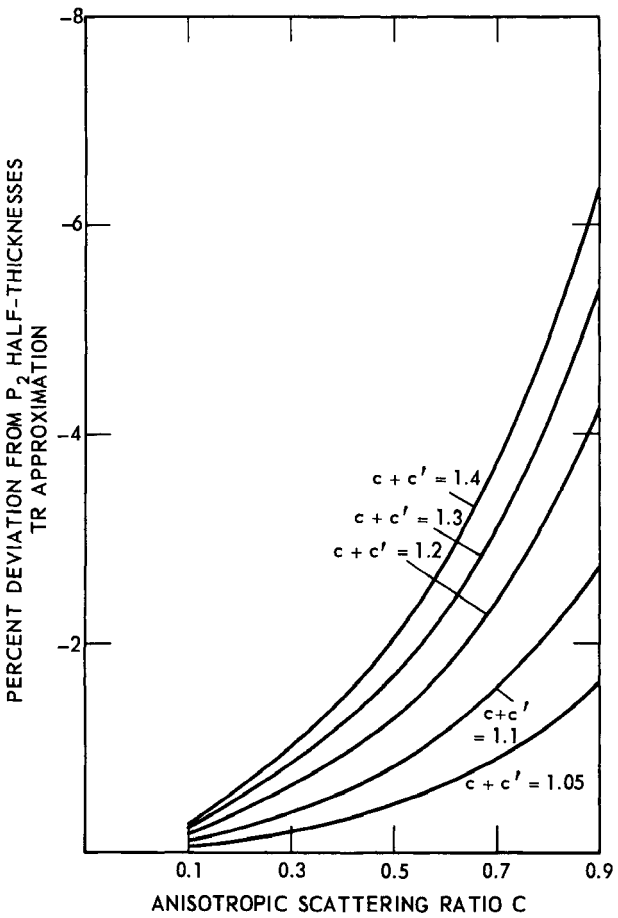

Fig. 9. Percentage deviation from P_2 critical half-thicknesses as a function of the anisotropic scattering ratio. TRANSPORT approximation.

P_1 approximation, which underestimates λ_0 for $c + c' > 1$, overestimates the critical half-thickness as shown in Fig. 10. In both approximations the errors are greatest for the largest values of c and $c + c'$. When $c + c'$ is large the critical slab is quite small, and leakage ('transient' boundary) effects are more important. As could be anticipated from the plane source problem results, the *TR* and P_1 approximation results are poorest in these situations.

The good agreement of P_2 and P_4 fluxes, eigenvalues and half-thicknesses is somewhat surprising considering the nature of the hydrogen scattering function. To provide a more difficult test of P_N approximations, discrete eigenvalues were calculated using the scattering function $f(\mu_0) = \exp(10\mu_0)$ of Francis, *et al.*[13]. Table X displays λ_0 for three P_N approximations. The P_9 results given in Table X agree with those given in Ref. 13. Considering the extremely anisotropic nature of the scattering and the slow decrease of the b_n coefficients, the agreement of the P_3 approximation results is very good. The implication is that rela-

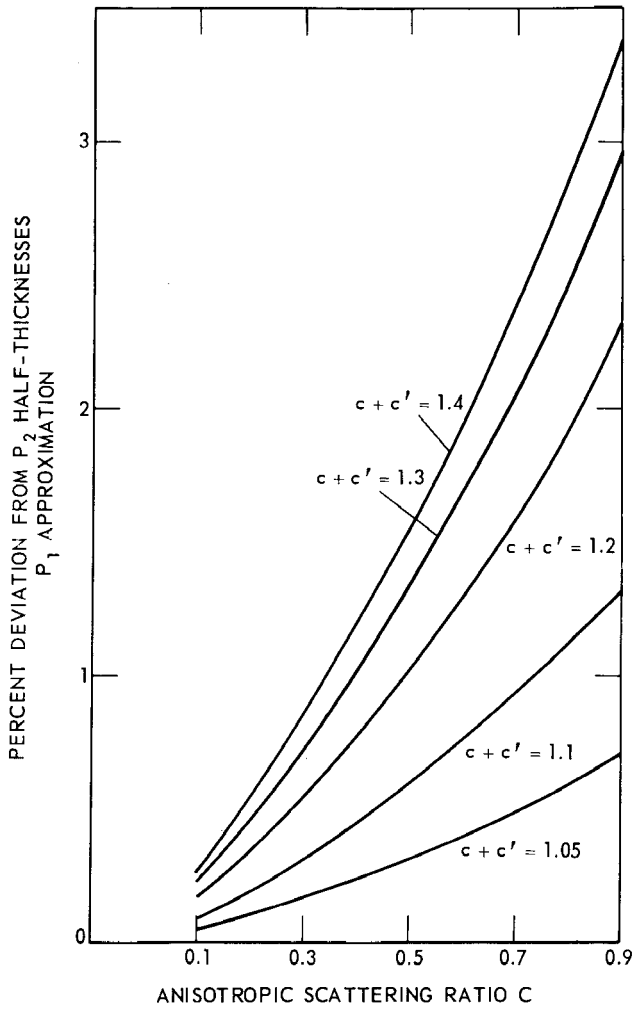

Fig. 10. Percentage deviation from P_2 critical half-thicknesses as a function of the anisotropic scattering ratio. P_1 approximation.

tively low order P_N (N = 2 or 3) approximations are adequate to represent even severe anisotropic scattering when integral quantities are of interest. However, the detailed representation of the angular flux is another matter, since the results of Ref. 13 required a much higher order P_N *flux* representation for good accuracy. The above conclusions are substantiated in part by calculations of the photon flux in iron media. At high photon energies the scattering transfer is strongly biased in the forward direction, so much so that the coefficients of the Legendre scattering components scarcely decrease with increasing N. In several test problems P_3 and P_5 fluxes and leakages differed only slightly and results of both approximations agreed well with Monte Carlo results.

SUMMARY

In general, for computational purposes, the P_N approximations are more accurate than the corresponding alterations. That is, the P_1 approximation is more accurate than the *TR* approximation and the P_2 approximation more accurate than the *EXTR* approximation. The *TR* approximation is to be avoided whenever anisotropic scattering is important or whenever the detailed behavior of the flux is significant. That is not to say that the *TR* approximation does not have a wide range of applicability, for in many situations $c + c'$ is near unity, or the concentrations of the anisotropic scatter are small, or the angular flux is nearly isotropic and the *TR* approximation can be used with good accuracy. In most cases of practical interest the *EXTR* approximation should offer a convenient and accurate modification of the P_1 approximation. The tables and figures above and their counterparts in Ref. 7 provide a guide to the use of anisotropic scattering approximations.

[12]G. J. MITSIS, "Transport Solutions to the Monoenergetic Critical Problems," Argonne National Laboratory Report ANL-6787 (1963).

[13]N. C. FRANCIS, E. J. BROOKS and R. A. WATSON, *Trans. Am. Nucl. Soc.*, **6**, 283 (1963).

TABLE X

Discrete Eigenvalues for Severe Anisotropic Scattering

Anisotropic Scattering Ratio c	P_2 Scattering Approximation	P_3 Scattering Approximation	P_9 Scattering Approximation	n	Scattering Coefficient b_n
0.1	0.98927	0.98054	0.97260	1	0.9
0.2	0.93701	0.91917	0.90975	2	0.73
0.3	0.86168	0.84129	0.83363	3	0.535
0.4	0.77356	0.75435	0.74899	4	0.355
0.5	0.67670	0.66075	0.65746	5	0.21505
0.6	0.57284	0.56118	0.55945	6	0.118945
0.7	0.46242	0.45523	0.45452	7	0.064215
0.8	0.34443	0.34115	0.34096	8	0.0283127
0.9	0.21426	0.21353	0.21352	9	0.0122899